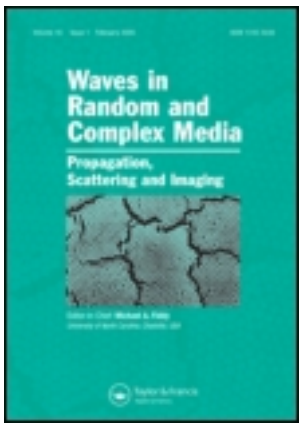

Waves in Random Media
Publication details, including instructions for authors and subscription information:
http://www.tandfonline.com/loi/twrm19

Elastic waves in non-Newtonian (Maxwell) fluid-saturated porous media

Zhi-Wen Cui [a] , Jin-Xia Liu [a] & Ke-Xie Wang [a]
[a] Department of Acoustics and Microwaves, Physical Institute, Jilin University, JieFang Road No 119, 130023, ChangChun, People's Republic of China

Version of record first published: 15 Aug 2006

To cite this article: Zhi-Wen Cui, Jin-Xia Liu & Ke-Xie Wang (2003): Elastic waves in non-Newtonian (Maxwell) fluid-saturated porous media, Waves in Random Media, 13:3, 191-203

To link to this article: http://dx.doi.org/10.1088/0959-7174/13/3/304

INSTITUTE OF PHYSICS PUBLISHING WAVES IN RANDOM MEDIA

Waves Random Media **13** (2003) 191–203 PII: S0959-7174(03)57544-9

Elastic waves in non-Newtonian (Maxwell) fluid-saturated porous media

Zhi-Wen Cui[1], **Jin-Xia Liu and Ke-Xie Wang**

Department of Acoustics and Microwaves, Physical Institute, Jilin University, JieFang Road No 119, 130023, ChangChun, People's Republic of China

E-mail: zwcuijlu@sohu.com and liuacoustics@mail.china.com

Received 17 December 2002, in final form 22 May 2003
Published 18 June 2003
Online at stacks.iop.org/WRM/13/191

Abstract

This paper studies the elastic waves in non-Newtonian (Maxwell) fluid-saturated porous media with the nonzero boundary slip velocity for pore size distribution. The coefficient $bF_m(\omega)$ that measures the deviation from Poiseuille flow friction in such media is presented. Based on this coefficient, we investigate the properties of elastic waves by calculating their phase velocities and attenuation coefficients as functions of frequency and the behaviour of the dynamic permeability. The study shows that the pore size distribution removes oscillations in all physical quantities in the non-Newtonian regime. Consideration of the nonzero boundary slip effect in non-Newtonian (Maxwell) fluid-saturated porous media results in (a) an overall increase of the dynamic permeability, (b) an increase of phase velocities of fast Biot waves and shear waves except in the low frequency domain and an overall increase of phase velocity of slow Biot waves and (c) an overall increase of the attenuation of three Biot waves in the intermediate frequency domain except in the deeply non-Newtonian regime. The study also shows that the attenuation coefficient of slow Biot waves is small in the deeply non-Newtonian regime at higher frequency, which encourages us to detect slow Biot waves in oil-saturated porous rock.

1. Introduction

The physics of elastic wave propagation in fluid-saturated porous media has for a very long time captured the interest of many investigators in exploration seismology, petroleum geophysics, soil engineering, underwater acoustics and foundation engineering. Elastic wave propagation measurements are useful and convenient tools for investigating the inner properties of fluid-saturated porous media. In the theory of elastic wave propagation through porous media, acoustic velocity and attenuation in sediments and porous rocks are related to physical properties of the material. Understanding the whole mechanism involved in acoustic energy dissipation and velocity dispersion during the passage of an elastic wave is an important and

[1] Author to whom any correspondence should be addressed.

0959-7174/03/030191+13$30.00

interesting problem of acoustics and geophysics. Moreover, in petroleum geophysics, regional exploration seismology needs direct methods of discovering oil-filled rocks, which should be based on models of propagation of elastic waves in porous media with realistic fluid.

The theory of elastic wave propagation in fluid-saturated porous media was first considered by Biot [1] directly at macroscopic level. Biot's theory of elastic wave propagation in porous materials is the general framework for studying the effects of fluid movement into and out of each element of porous material during the passage of elastic waves. Biot predicts the existence of two kinds of compressional (P) wave in a fluid-saturated porous medium: the fast P wave (P1 wave) for which the solid and fluid displacements are in phase, and the slow P wave (P2 wave) for which displacements are out of phase. The slow P wave in water-saturated sintered glass beads was observed first by Plona [2], and recently this wave has been observed for the first time in natural water-saturated Nivelsteiner sandstone [3]. Biot's theory has been a successful tool for interpreting experimental data for decades, and has been applied in fields as diverse as geophysics and bone [4].

However, there are many examples of real earth materials for which Biot's theory does not seem to explain the dispersion and attenuation very well. Various additions and corrections to Biot's theory have been attempted including treating the pore fluid as gel [5], considering the effects of pore size distribution [5, 6], combining the squirt flow mechanism with Biot's mechanism [7], considering the effects of nonzero boundary slip velocity [8] and so on. For a classic Newtonian fluid, those extended Biot theories can be used to describe interaction of fluid-saturated solid with the sound. But for oil and other hydrocarbons, often exhibiting significant non-Newtonian behaviour, they are not appropriate again. Recently, Tsiklauri and Beresnev [9] treated the pore fluid as a non-Newtonian (Maxwell) fluid and studied the properties of elastic wave propagation in such fluid-saturated porous media [10]. In [9, 10], Tsiklauri and Beresnev only considered all cylindrical pores of the same size with a no-slip boundary, and their studies show that there is oscillation on curves of physical quantities. Note that in [8] there is an overall decrease of the phase velocities of P1 and shear waves.

The purpose of this paper is to study properties of the elastic wave propagation in non-Newtonian (Maxwell) fluid-saturated porous media. As a step forward, the novelty in the present work is that we combine models of Tsiklarui [8], which introduced nonzero boundary slip velocity, and Tsiklauri and Beresnev [9, 10], which introduced non-Newtonian effects into the classic Biot theory, into a single more general model for an arbitrary distribution of pore size. It is more realistic that pores have some distribution of radii. We generalize the expression for the function $bF_m(\omega)$, which measures the deviation from Poisseuille flow friction as a function of frequency. Based on this generalized Biot–Tsiklauri model, we investigated the elastic waves in non-Newtonian (Maxwell) fluid-saturated porous media with pore size distribution by calculating their phase velocities and attenuation coefficients as a function of frequency. We also investigated the behaviour of the dynamic permeability as a function of frequency. The results of the present paper may be of interest for researchers in the field referred to above as well as experimental wave propagation in fluid-saturated porous media.

The paper is organized as follows. In section 2, we formulate a theoretical basis for the generalized Biot–Tsiklauri model. The numerical results are shown in section 3, and our discussions are given in the last section.

2. The model

We consider the model of a Maxwell fluid flowing in a cylindrical tube whose walls are oscillating longitudinally and the fluid is subject to an oscillatory pressure gradient. We give analytical solutions to the problem in the frequency domain. We describe the viscoelastic

effect of the fluid using Maxwell's model, which assumes that

$$t_m \frac{\partial \boldsymbol{\tau}}{\partial t} = -\eta \nabla \boldsymbol{v} - \boldsymbol{\tau} \tag{1}$$

where η is the viscosity coefficient, t_m is the relaxation time (hereafter m denotes Maxwell) and $\boldsymbol{v}$ denotes the velocity of the fluid, whereas $\boldsymbol{\tau}$ represents the viscous stress tensor. In the present paper, all quantities that are sinusoidal functions of time contain a factor $\exp(-\mathrm{i}\omega t)$, where ω is angular frequency, so

$$\boldsymbol{\tau} = -\eta \nabla \boldsymbol{v}/(1 - \mathrm{i}\omega t_m). \tag{2}$$

Under the assumption that the local relative flow is incompressible ($\nabla \cdot \boldsymbol{v} = 0$), the equation of motion of the fluid is

$$\rho_f \frac{\partial \boldsymbol{v}}{\partial t} = -\nabla p + \eta \nabla^2 \boldsymbol{v}/(1 - \mathrm{i}\omega t_m) \tag{3}$$

where ρ_f and p are the density and pressure of the fluid, respectively. Next, the average force exerted by fluid on the solid in the direction of motion is obtained.

Following Biot [1], we consider the motion of Maxwell fluid in a three-dimensional duct. The z-direction is parallel to the boundaries, so the flow of fluid in a duct can be described by a single component of velocity, i.e. $\boldsymbol{v} = v(r)\boldsymbol{e}_z$. In the cylindrical coordinate system (r, θ, z), with the relative velocity $U_1(r) = v(r) - \dot{u}$, where $\dot{u}$ is the velocity of the duct, we can write equation (3) as

$$\nabla^2 U_1 + \beta^2 U_1 = -X \frac{\beta^2}{\mathrm{i}\omega}; \tag{4}$$

here $X = -\frac{1}{\rho_f}\nabla p - \frac{\partial \dot{u}}{\partial t}$ is an external volume force [1, 8], and $\beta^2 = (\omega^2 t_m + \mathrm{i}\omega)\rho_f/\eta$.

In light of the recent experimental results in [11], following Tsiklauri [8], we can assume a boundary slip velocity on the wall of the duct with the diameter of $2a$, and then obtain

$$U_1(r) = -\frac{X}{\mathrm{i}\omega}\left[1 - \frac{(1 + \bar{U}_s)J_0(\beta r)}{J_0(\beta a)}\right]. \tag{5}$$

$\bar{U}_s$ takes the expression of Tsiklauri [8], so it will not be repeated here. Thus we can find the cross-section-averaged velocity [1, 9] (J_0 and J_1 are the Bessel functions)

$$\bar{U}_1(a) = -\frac{X}{\mathrm{i}\omega}\left[1 - \frac{2(1 + \bar{U}_s)J_1(\beta a)}{\beta a J_0(\beta a)}\right]. \tag{6}$$

Thus, from (2) the total friction force per unit cross section of the duct can be derived as

$$\frac{2\tau}{a} = \frac{X}{\mathrm{i}\omega}\frac{\eta}{1 - \mathrm{i}\omega t_m}\frac{2(1 + \bar{U}_s)\beta J_1(\beta a)}{a J_0(\beta a)}. \tag{7}$$

The fluid cross section occupies a fraction ϕ (porosity) of the cross section of the bulk material, so the friction per unit bulk volume is

$$\phi\frac{2\tau}{a} = \phi\frac{X}{\mathrm{i}\omega}\frac{\eta}{1 - \mathrm{i}\omega t_m}\frac{2\beta(1 + \bar{U}_s)J_1(\beta a)}{a J_0(\beta a)}. \tag{8}$$

In the present paper, we consider the characteristic pore size with arbitrary distribution, which may be applicable to a wide variety of actual materials, just as Biot [1] has pointed out. Some authors [5, 6] have studied the effects of the pore size distribution on the elastic wave in a fluid-saturated and a gel-saturated porous medium, respectively. Assuming a group of

capillary tubes with a radial probability density distribution function $f(a)$ with a total porosity ϕ, we can express the average force exerted by fluid on the solid as

$$\int_0^\infty \phi \frac{2\tau}{a} f(a)\,\mathrm{d}a = \frac{X}{\mathrm{i}\omega} \frac{\eta}{1-\mathrm{i}\omega t_m} \int_0^\infty \phi \frac{2\beta(1+\bar{U}_s)J_1(\beta a)}{a J_0(\beta a)} f(a)\,\mathrm{d}a. \tag{9}$$

The average $\bar{U}_1(a)$ is

$$\int_0^\infty \bar{U}_1(a) f(a)\,\mathrm{d}a = K(\omega)X = \frac{X}{\mathrm{i}\omega}\left\{\int_0^\infty \left[\frac{2(1+\bar{U}_s)J_1(\beta a)}{\beta a J_0(\beta a)} - 1\right] f(a)\,\mathrm{d}a\right\} \tag{10}$$

where $K(\omega)$ is the dynamic permeability [9, 12] that describes the frequency dependent response of the tube to the applied total force on the fluid. The concept of dynamic permeability has been widely used in other papers [13, 14].

For this section, we presume familiarity with the contents of Biot's theory [1, 15]. In Biot's theory, to evaluate $bF(\omega)$ we remember that it is the ratio of the total friction force between the fluid and the solid to the average relative velocity per unit volume of bulk material. This coefficient can be obtained from (9) and (10) as

$$bF_m(\omega) = \mathrm{i}\omega\phi\rho_f \frac{Z(\omega)}{Z(\omega)-1} \tag{11}$$

where $Z(\omega) = \int_0^\infty \frac{2(1+\bar{U}_s)J_1(\beta a)}{\beta a J_0(\beta a)} f(a)\,\mathrm{d}a$. We only need to replace $bF(\omega)$ with $bF_m(\omega)$ in Biot's equation, so we can apply Biot's theory to non-Newtonian (Maxwell) fluid-saturated porous media. Similarly, the viscosity correction factor F_m is defined by comparing a physical quantity of the oscillatory flow with that of the Poiseuille flow.

$$F_m(\omega) = \mathrm{i}\frac{\omega}{\omega_c}\frac{Z(\omega)}{Z(\omega)-1}. \tag{12}$$

$F_m(\omega)$ measures the deviation from Poiseuille flow friction as a function of the frequency [1, 9]. $\omega_c = \phi\eta/\rho_f\kappa_0$ is Biot's transition frequency. κ_0 is the effective permeability of porous media, which can be obtained by $\kappa_0 = \int_0^\infty (\phi/8)a^2 f(a)\,\mathrm{d}a$.

When $t_m = 0$ and $\bar{U}_s = 0$, this study corresponds to the generalized Biot theory with pore size distribution developed by Yamamoto [6]; when $t_m = 0$, all pores are of the same size and $\bar{U}_s \neq 0$, this study corresponds to that of Tsiklauri [8]; when all pores are of the same size, and $\bar{U}_s = 0$, this study corresponds to that of Tsiklauri and Beresnev [9]; if all pores have the same size, $t_m = 0$ and $\bar{U}_s = 0$, this study corresponds to that of Biot [1].

The general equations that govern propagation of elastic waves in non-Newtonian (Maxwell) fluid-saturated porous media are

$$\begin{aligned} &\mu_b\nabla^2\boldsymbol{u} + (H-\mu_b)\nabla\nabla\cdot\boldsymbol{u} + C\nabla\cdot\boldsymbol{w} = \frac{\partial^2}{\partial t^2}(\rho\boldsymbol{u} + \rho_f\boldsymbol{w}) \\ &\nabla(C\nabla\cdot\boldsymbol{u} + M\nabla\cdot\boldsymbol{w}) = \frac{\partial^2}{\partial t^2}(\rho_f\boldsymbol{u} + \rho_m\boldsymbol{w}) \end{aligned} \tag{13}$$

where H, C, M are the generalized elastic coefficients deduced by Biot and expressed as

$$\begin{aligned} H &= K_b + 4\mu_b/3 + (1-K_f/K_s)C, \\ C &= (1-K_f/K_s)M, \\ M &= K_f K_s/[\phi K_s + (1-K_f/K_s-\phi)K_f] \end{aligned} \tag{14}$$

and K_s, K_f, K_b and μ_b denote the solid grain modulus, pore fluid bulk modulus, framework modulus and shear modulus. These quantities are measurable for a porous medium. $\boldsymbol{w} = \phi(\boldsymbol{u}_f - \boldsymbol{u})$ represents the flow of the fluid relative to the solid and is measured in terms of volume per unit area of the bulk medium, where $\boldsymbol{u}_f$ and $\boldsymbol{u}$ are the absolute displacements of

the pore fluid and solid phase of a porous medium, respectively. The density of bulk can be expressed by the density of grain ρ_s and the density of pore fluid ρ_f as $\rho = (1-\phi)\rho_s + \phi\rho_f$. $\rho_m = \mathrm{i}\eta/\omega\kappa(\omega)$ is the effective density of the fluid in relative motion. Biot's dynamic permeability $\kappa(\omega)$ [14] can be expressed as

$$\kappa(\omega) = \kappa_0[F_m(\omega) - \mathrm{i}\omega/\omega_c]^{-1} = \frac{\mathrm{i}}{\omega}(1-Z)\phi\frac{\eta}{\rho_f} = \phi\frac{\eta}{\rho_f}K(\omega). \tag{15}$$

Here $\kappa(\omega)$ describes the response of the fluid-saturated porous medium to an applied stimulus, and characterizes the frequency-dependent behaviour of pore fluid flow. We can find a comprehensive and detailed discussion of the dynamic permeability in [13, 14].

The velocity and attenuation of Biot's waves are

$$V_j = 1/\operatorname{Re}\sqrt{Y_j}, \qquad Q_j^{-1} = 2\operatorname{Im}\sqrt{Y_j}/\operatorname{Re}\sqrt{Y_j} \qquad j = \mathrm{P1}, \mathrm{P2}, \mathrm{s} \tag{16}$$

where P1 and P2 denote compressional waves of the first kind and second kind, respectively, and s denotes a shear wave.

For P1 and P2 waves, Y is determined by the quadratic equation

$$c_2Y^2 - c_1Y + c_0 = 0 \tag{17}$$

where

$$c_2 = HM - C^2, \qquad c_1 = H\rho_m + M\rho - 2\rho_f C, \qquad c_0 = \rho\rho_m - \rho_f^2;$$

for the shear waves, Y_s is determined by

$$Y_s^2 = (\rho - \rho_f^2/\rho_m)/\mu_b. \tag{18}$$

3. Numerical results

In the following, we calculated normalized phase velocities of three Biot waves V_{P1}/V_C, V_{P2}/V_C and V_s/V_t and the attenuation coefficients as well as dynamic permeability using our more general expression for $F_m(\omega)$ given by equation (12). The velocities V_{P1} and V_s tend to $V_C = \sqrt{H/\rho}$ and $V_t = \sqrt{\mu_b/\rho}$ for zero frequency respectively. Pore radii of porous media, for example a certain carbonate rock [16], can be approximated by a log normal distribution $N(\log a, \sigma^2)$. The pore radius probability density distribution function is

$$N(\log a) = \frac{1}{\sqrt{2\pi}\sigma}\exp\left[-\frac{(\log a - \log a_\mu)^2}{2\sigma^2}\right] \tag{19}$$

where $\log a_\mu$ and σ^2 are the mean and variance of log-transformed pore radius ($\log a$) respectively. a_μ is the median pore radius.

We select the parameters as in [17]: $K_f = 2.25$ GPa, $K_s = 35.7$ GPa, $K_b = 14.39$ GPa, $\mu_b = 13.99$ GPa, $\rho_f = 1000$ kg m^{-3}, $\rho_s = 2650$ kg m^{-3}, $\phi = 0.2$, $\eta = 0.001$ Pa s and $a_\mu = 7.5$ μm. Our selected elastic constants from [17] are for a typical sand rock. As in [6], we can obtain the permeability by $\kappa_0 = \frac{\phi}{8}a_\mu^2\exp[2(\sigma\ln 10)^2]$. $\sigma = 0$ corresponds to the case where all pore radii have the same size. Here, we use De to denote the Deborah number, which is defined as the ratio of the characteristic time viscous effect $t_v = a_\mu^2\rho_f/\eta$ to the relaxation time t_m, i.e., $De = t_v/t_m$. It is the Deborah number that determines in which regime the system resides. For a small De, the system exhibits a viscoelastic behaviour, which we call the non-Newtonian regime.

In figure 1 with $\sigma = 0$ we plot phase velocities for six different cases: the thick solid curve corresponds to $\xi = 0$, $De = \infty$ i.e., no-slip boundary and Newtonian fluid-saturated case (Biot's model), the long dashed curve corresponds to $\xi = 0.5$, $De = \infty$ (Tsiklauri model [8],

ξ is the weight factor of the boundary slip effect), the short dashed curve corresponds to $\xi = 0.0$, $De = 10$ (Tsiklauri–Beresnev model [9, 10]), the dash–dot–dot curve corresponds to $\xi = 0.5$, $De = 10$, the dotted curve corresponds to $\xi = 0.0$, $De = 1$ (Tsiklauri–Beresnev model) and the thin solid curve corresponds to $\xi = 0.5$, $De = 1$. The last two cases correspond to the deeply non-Newtonian regime. From figures 1(a) and (c), we can find that the introduction of the slip boundary into the non-Newtonian (Maxwell) fluid-saturated porous media results in phase velocities of P1 and shear waves settling at a somewhat lower value than those in the no-slip-boundary case at low frequencies. However, there is an increase of phase velocities of P1 and shear waves except at low frequencies in contrast to the decrease of phase velocities in Newtonian fluid-saturated porous media (also see [8]). We also can find that phase velocities of P1 and shear waves are somewhat smaller in value than those in the Newtonian fluid-saturated case at lower frequencies. From figure 1(b) we notice that there is an increase of phase velocity of P2 waves at all frequencies. The introduction of the slip boundary into non-Newtonian (Maxwell) fluid-saturated porous media results in the phase velocity of P2 waves settling at a somewhat higher value than those in no-slip-boundary cases, which is similar to [9, 10]. Here we notice the appearance of sharp oscillatory curves in the deeply non-Newtonian regime, which means that the wave has entered the non-Newtonian regime.

In figure 2 we plot the attenuation of P1, P2 and shear waves as a function of frequency for six cases as in figure 1. We notice that the attenuation coefficients settle at higher values in non-Newtonian fluid-saturated porous media with slip boundary ($\xi \neq 0$) than those in no-slip-boundary cases. The attenuations in the deeply non-Newtonian regime (both slip and no-slip boundary cases) are much higher than those in the Newtonian fluid-saturated case at lower frequencies, which comes to our notice even in the general non-Newtonian regime ($De = 10$). The pronounced oscillatory curves in the deeply non-Newtonian regime can be noticed again.

In figure 3 we plot the value of dynamic permeability as a function of frequency for six cases as in figure 1. We observe that non-Newtonian effects cause substantial enhancements in dynamic permeability, and slip boundary effects enhance the value of dynamic permeability for all cases. The oscillatory curves in the deeply non-Newtonian regime can be noticed again. In figures 1–3, the appearance of oscillation in the curves is due to non-Newtonian effects.

In figure 4 we plot the velocities corresponding to six different cases as in figure 1. In one case, we consider the effect of pore size distribution, which is more realistic than the cases where all pores have the same size. We choose $\sigma = 0.2$ and only consider the non-Newtonian effects and the slip boundary effects because the attenuation and velocity characteristics of three Biot waves in such porous media becomes strongly dependent on the pore size distribution as discussed by Yamamoto and Turgut [6]. From figure 4 we can observe that there is no sharp oscillation on curves in non-Newtonian fluid-saturated porous media. Oscillations are removed due to weighted superposition of different pore radii based on $Z(\omega)$. From figures 4(a) and (c) we can find that the introduction of the slip boundary into the non-Newtonian (Maxwell) fluid-saturated porous media results in phase velocities of P1 and shear waves settling at a somewhat lower value than those in the no-slip-boundary case at low frequencies; however, there is an increase of phase velocities of P1 and shear waves except at low frequencies in contrast to the decrease of phase velocities in Newtonian fluid-saturated porous media (also see [8]). From figure 4(b) we notice that there is an increase of phase velocity of P2 waves at all frequencies. The introduction of the slip boundary into non-Newtonian (Maxwell) fluid-saturated porous media results in the phase velocity of P2 waves settling at somewhat a higher value than the no-slip-boundary cases, which is similar to [10]. The phase velocities of P1 and shear waves somewhat smaller in value than those in the Newtonian fluid-saturated case at lower frequencies can be observed again.

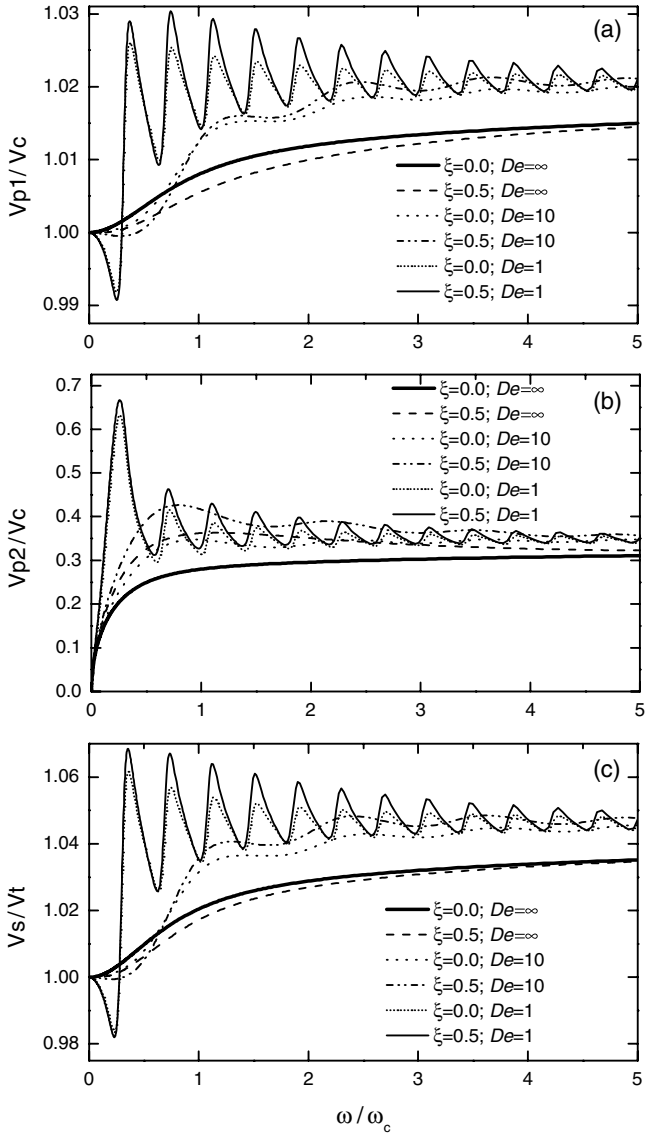

Figure 1. Behaviour of the normalized phase velocity of the P1, P2 (compressional wave of the first kind and compressional wave of the second kind) and shear waves as a function of frequency for six cases. (a) P1 waves; (b) P2 waves; (c) shear waves. The thick solid curve corresponds to the case $\xi = 0$, $De = \infty$ i.e. no-slip-boundary and Newtonian fluid-saturated case (Biot's model), the long dashed curve corresponds to $\xi = 0.5$, $De = \infty$ (Tsiklauri's model), the short dashed curve corresponds to $\xi = 0.0$, $De = 10$ (Tsiklauri–Beresnev model), the dash–dot–dot curve corresponds to $\xi = 0.5$, $De = 10$, the dotted curve corresponds to $\xi = 0.0$, $De = 1$ (Tsiklauri–Beresnev model) and the thin solid curve corresponds to $\xi = 0.5$, $De = 1$, respectively. All cases correspond to $\sigma = 0$ (no pore size distribution).

In figure 5 we plot the attenuation coefficients with pore size distribution as in figure 4. We also find that the sharp oscillatory curves in figure 2 disappear, which is due to weighted superposition of different pore radii based on $Z(\omega)$. Introducing the slip boundary into non-Newtonian fluid-saturated porous media results in the attenuation of Biot's waves settling at

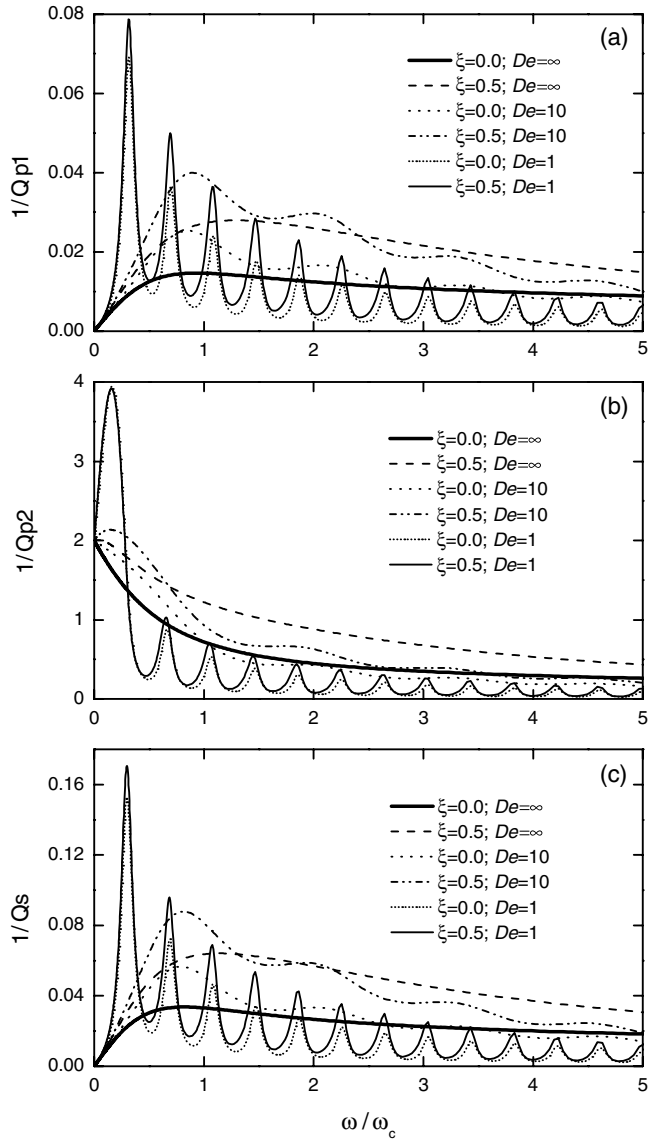

Figure 2. Attenuation coefficient of the P1, P2 and shear waves as a function of frequency for six cases as in figure 1. (a) P1 waves; (b) P2 waves; (c) shear waves. All cases correspond to $\sigma = 0$ (no pore size distribution).

a somewhat higher value than those in the no-slip boundary case. In the lower frequency domain, the attenuation values of Biot's waves are obviously much higher than those predicted by Biot's model. The attenuation of the P2 wave in the deeply non-Newtonian regime is much smaller than that in Newtonian fluid-saturated porous media in the higher frequency domain.

In figure 6 we plot the value of dynamic permeability with pore size distribution for six cases as in figure 3. The results show that oscillations on curves disappear, due to weighted superposition of different pore radii based on $Z(\omega)$ and both the slip boundary effect and non-Newtonian effect result in enhancement of dynamic permeability. In figure 7 we plot the value of dynamic permeability for the very deeply non-Newtonian regime ($De = 0.1$); we can

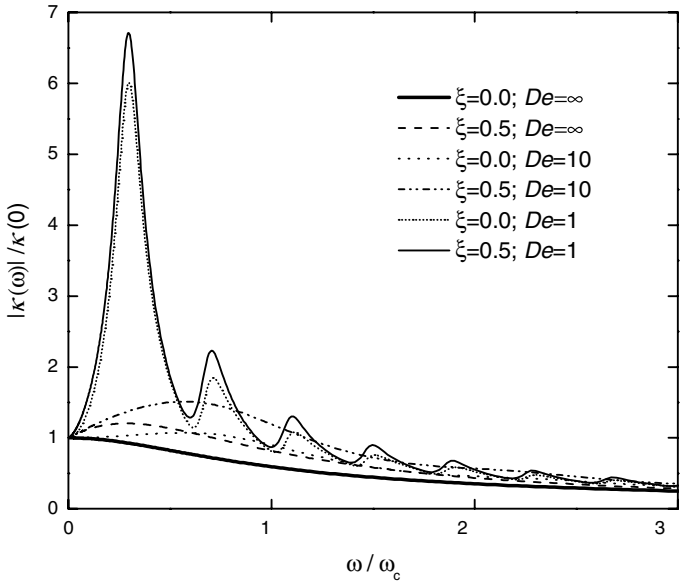

Figure 3. Behaviour of normalized dynamic permeability $|\kappa(\omega)|/\kappa(0)$ as a function of frequency for six cases as in figure 1. All cases correspond to $\sigma = 0$ (no pore size distribution).

obtain an increase in permeability of up to about seven times at certain resonant frequencies, that of slip boundary case is only slightly higher than that of no slip boundary occurred. As Tsiklauri and Beresnev [9] pointed out, in crude oil, there are certain resonant frequencies at which oil production can be increased significantly if the well is irradiated with elastic waves at those frequencies.

4. Discussions

In the present paper, as a step forward, we have combined models by Tsiklarui [8], which introduced *nonzero boundary slip velocity*, and Tsiklauri and Beresnev [9, 10], which introduced *non-Newtonian effects* into the classic Biot theory, into a single more general model *for an arbitrary distribution of pore size*. We derived the coefficient $bF_m(\omega)$ that measures the deviation from Poiseuille flow friction by including the pore size distribution, nonzero boundary slip velocity and non-Newtonian effects. It is convenient to replace $bF(\omega)$ by $bF_m(\omega)$ in Biot's equations in order to study the properties of elastic waves in non-Newtonian (Maxwell) saturated porous media. We have studied the properties of the elastic wave propagation in non-Newtonian (Maxwell) fluid-saturated porous media with pore size distribution by calculating their phase velocities and attenuation coefficients as a function of frequency. We also investigated the behaviour of the dynamic permeability as a function of frequency.

For the cases of all pores having the same size, the appearance of oscillation in curves (figures 1–3) is due to non-Newtonian effects based on equation (12), that has been derived for pore fluid as a Maxwell fluid. However, we cannot confirm that such strong oscillatory phenomena should be attributed to the non-Newtonian effects, because they can appear in gel-saturated porous media due to gel behaviour in [5]. The two models have similar formulation, namely, the viscosity η is replaced by 'complex viscosity' $\eta(1 + \mathrm{i}\mu_g/\omega\eta)$ (μ_g is the shear rigidity of the gel) in the gel model [5] and the viscosity η is replaced by 'complex viscosity'

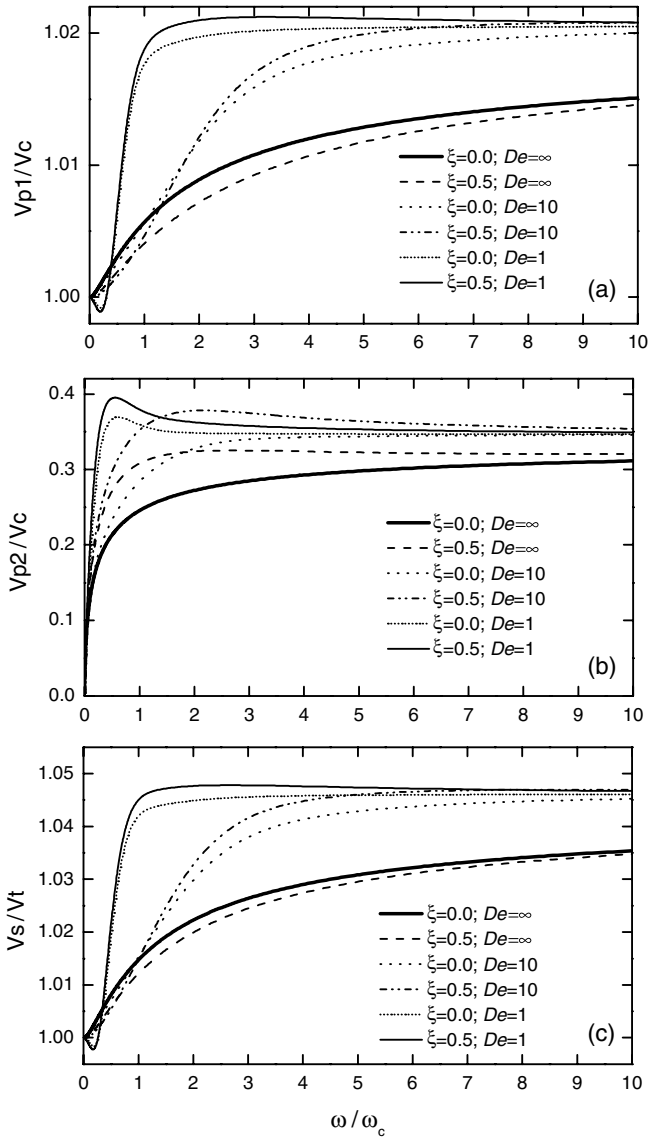

Figure 4. Behaviour of normalized phase velocity of the P1, P2 and shear waves as a function of frequency for six cases as in figure 1. (a) P1 waves; (b) P2 waves; (c) shear waves. Here, all cases correspond to $\sigma = 0.2$ (with pore size distribution).

$\eta/(1 - \mathrm{i}t_m\omega)$ in the Tsiklauri–Beresnev model [9, 10]. When $\omega \to \infty$, the gel model behaves as the classic Biot model [1]; when $\omega \to 0$, the Tsiklauri–Beresnev model behaves as the classic Biot model. But this study shows that the non-Newtonian effect is another important attenuation and velocity dispersion mechanism of elastic waves in saturated porous media.

The inclusion of *pore size distribution* in our general Biot–Tsiklauri model *removes oscillations in the physical quantities in the non-Newtonian regime*, *even in the deeply non-Newtonian regime*. Because of weighted superposition of different pore radii based on $Z(\omega)$, oscillations in the physical quantities are removed. It is *more realistic* to suppose that the pores have some distribution of radii, naturally in accord with the view of statistical physics.

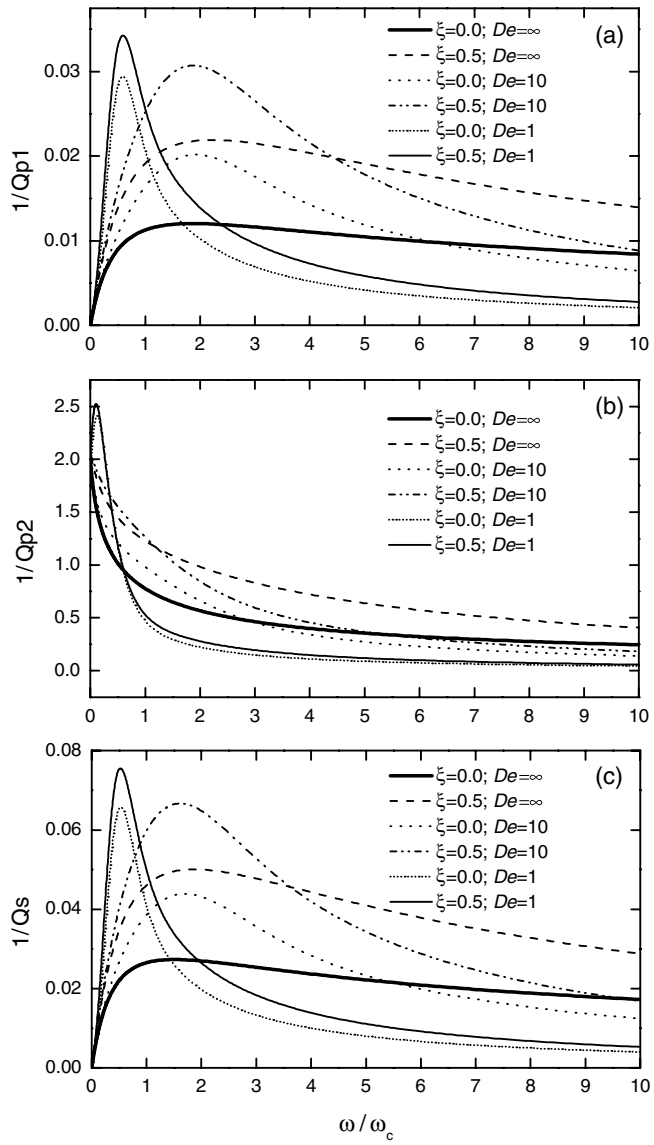

Figure 5. Attenuation coefficient of the P1, P2 and shear waves as a function of frequency for six cases as in figure 1. (a) P1 waves; (b) P2 waves; (c) shear waves. Here, all cases correspond to $\sigma = 0.2$ (with pore size distribution).

The combination of nonzero slip boundary and non-Newtonian effects results in

(a) an *overall increase* of the *dynamic permeability*,
(b) an *increase* of *phase velocities* of fast Biot waves and shear waves except in the low frequency domain and an overall increase of phase velocity of slow Biot waves and
(c) an *overall increase of the attenuation* of three Biot waves in the intermediate frequency domain except for the deeply non-Newtonian regime.

Apart from other mechanisms, combination of nonzero boundary slip and non-Newtonian effects is a *valid physical mechanism* for energy loss, and may be responsible for the deviations

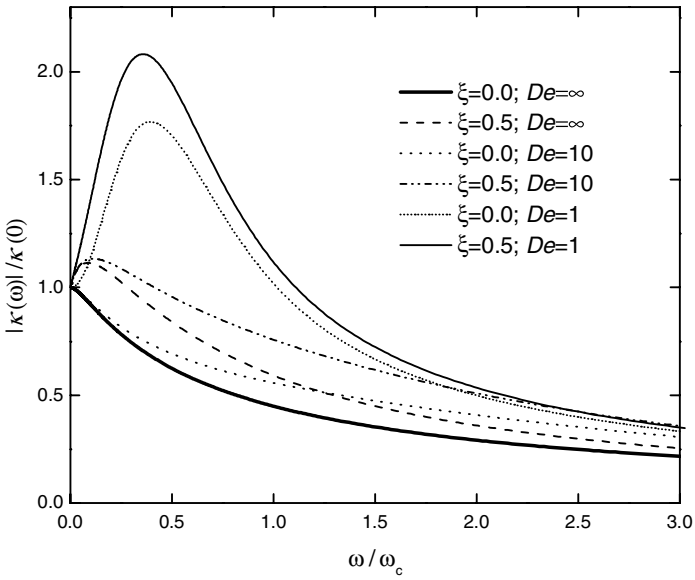

Figure 6. Behaviour of normalized dynamic permeability $|\kappa(\omega)|/\kappa(0)$ as a function of frequency for six cases as in figure 1. Here all cases correspond to $\sigma = 0.2$ (with pore size distribution).

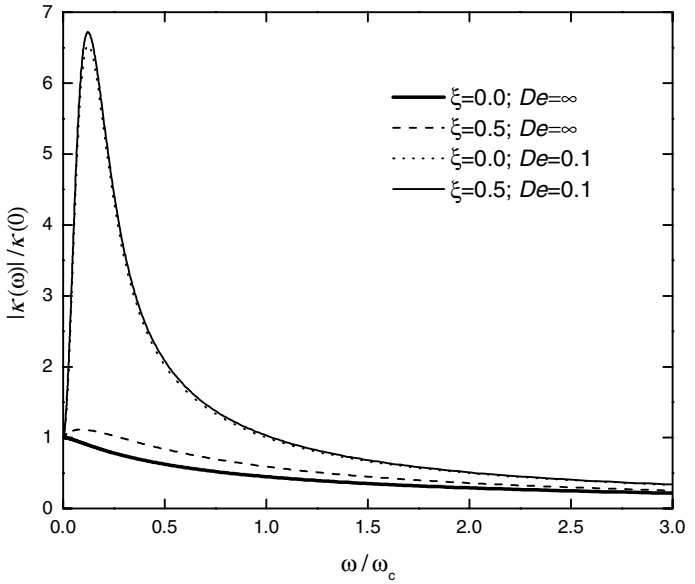

Figure 7. Behaviour of normalized dynamic permeability $|\kappa(\omega)|/\kappa(0)$ as a function of frequency for four cases in order to observe the effects of the deeply non-Newtonian regime. The thick solid curve corresponds to the case $\xi = 0$, $De = \infty$ (Biot), the long dashed curve corresponds to $\xi = 0.5$, $De = \infty$ (Tsiklauri), the short dashed curve corresponds to $\xi = 0.0$, $De = 0.1$ (Tsiklauri–Beresnev) and the thin solid curve corresponds to $\xi = 0.5$, $De = 0.1$. Here all cases correspond to $\sigma = 0.2$ (with pore size distribution).

between theory and experiment. The properties of velocity and attenuation may be used to explain experiment or field data. When other acoustic energy dissipation phenomena come

into play, other mechanisms (for example the 'squirt flow' mechanism [7]) have to be invoked to match the theory model to experimental data.

The results also show that it is of advantage to observe the slow Biot wave in the deeply non-Newtonian regime at higher frequency because of *smaller attenuation*. This encourages us to detect the Biot waves in crude-oil-saturated porous rock or cancellous bone. It may be easy to observe the Biot waves in porous media saturated with non-Newtonian (Maxwell) fluid by an experimental method.

The investigation of properties of elastic waves in fluid-saturated porous media is important for a number of applications. For example, in petroleum geophysics, regional exploration seismology needs an acoustic model to simulate acoustic logging waveforms, to estimate rock parameters (porosity, permeability) from borehole guided waves (e.g. Stoneley waves) and to discover oil-filled bodies of rocks. It should be based on models of propagation of elastic waves in porous media with *realistic fluid*. It is possible to correctly describe the process of elastic wave distribution in fluid-saturated porous media in the presence of an adequate model. Therefore, our generalized Biot–Tsiklauri model may be very useful.

However, the key limitation of this study is that the assumption of smooth capillary tubes does not capture the complexity of the sandstone pore geometry, and natural porous media, for example rocks, have a very different distribution of pore diameters. In the future work, we need to consider the effects of the *tortuosity* and '*squirt*' flow in order to mimic the natural porous media more realistically. Moreover, we also assume a boundary slip in a non-Newtonian fluid, and take the phenomenological expression for the boundary slip velocity of Tsiklauri's article [8]. As Tsiklauri pointed out, 'it may be possible to derive an expression based on more general "first principle", which should be a future work'.

Acknowledgments

This work was supported by the National Natural Science Foundation of China under grant No 40074032. The authors would like to thank Dr Wang Kun for her helpful discussions.

References

[1] Biot A M 1956a *J. Acoust. Soc. Am.* **28** 168
Biot A M 1956b *J. Acoust. Soc. Am.* **28** 179
[2] Plona T J 1980 *Appl. Phys. Lett.* **36** 259
[3] Kelder O and Smeulders D M J 1997 *Geophysics* **62** 1794
[4] Haire T J and Langton C M 1999 *Bone* **24** 291
[5] White J E and Wang KeXie 1989 *J. Acoust. Soc. Am.* **86** 1149
[6] Yamamoto T and Turgut A 1988 *J. Acoust. Soc. Am.* **83** 1744
[7] Dvorkin J and Nur A 1993 *Geophysics* **58** 524
[8] Tsiklauri D 2002 *J. Acoust. Soc. Am.* **112** 843
[9] Tsiklauri D and Beresnev I 2001 *Phys. Rev.* E **64** 036303
[10] Tsiklauri D and Beresnev I 2003 *Transp. Porous Media* **53** 39
[11] Zhu Y and Granick S 2001 *Phys. Rev. Lett.* **87** 096105
[12] del Rio J A, de Haro M L and Whitaker S 1998 *Phys. Rev.* E **58** 6323
[13] Johnson D L, Koplik J and Dashen R 1987 *J. Fluid Mech.* **176** 379
[14] Hu HengShan and Wang KeXie 2001 *Chin. J. Geophys.* **44** 135
[15] Biot A M 1962 *J. Appl. Phys.* **33** 1482
[16] Chen Q and Song Y Q 2002 *J. Chem. Phys.* **116** 8247
[17] Hu HengShan and Wang KeXie 2000 *Well Logging Technol.* **24** 3 (in Chinese)